

# Phosphor material evaluation for use in medical imaging radiation detectors by the noise-equivalent-quanta (NEQ) method

I. Kandarakis<sup>1</sup>, D. Cavouras<sup>1,\*</sup>, C.D. Nomicos<sup>2</sup>, G.S. Panayiotakis<sup>3</sup>

<sup>1</sup>Dept. of Medical Instrumentation Technology, Technological Educational Institution of Athens, Ag. Spyridonos Street, Aigaleo, 122 10 Athens, Greece

<sup>2</sup>Dept. of Electronics, Technological Educational Institution of Athens, Ag. Spyridonos Street, Aigaleo, 122 10 Athens, Greece

<sup>3</sup>Dept. of Medical Physics, Medical School, University of Patras, 265 00 Patras, Greece

Received: 11 August 1998/Revised version: 4 January 1999/Published online: 10 March 1999

**Abstract.** This study presents a method to evaluate the imaging performance of phosphor materials used in medical imaging systems. The advantage of the method is that phosphor evaluation is performed independently of the optical detectors (films, photocathodes, photodiodes) used in radiation detectors to capture phosphor light. The method is based on the noise-equivalent-quanta (NEQ) concept, which provides an index of the signal-to-noise ratio (SNR) associated with the diagnostic value of a medical image. NEQ was expressed as a function of the phosphor's emitted light wavelength, light energy flux, and modulation transfer function (MTF). All these parameters are related to intrinsic phosphor properties such as effective atomic number, density, activator ion. The method was tested on three yttrium-based phosphors, two of them activated with europium ( $\text{Eu}^{3+}$ ) and one with terbium ( $\text{Tb}^{3+}$ ). Results showed that europium-activated phosphors ( $\text{Y}_2\text{O}_2\text{S}:\text{Eu}$ ,  $\text{Y}_2\text{O}_3:\text{Eu}$ ) exhibited improved SNR, whereas the terbium phosphor ( $\text{Y}_2\text{O}_2\text{S}:\text{Tb}$ ) had better MTF.

**PACS:** 07.85; 42.30; 42.80

Phosphors are employed as X-ray or gamma-ray to light converters in detectors of medical imaging systems, such as radiographic cassettes, image intensifiers, gamma cameras, and digital radiography and computed tomography detectors. In all cases, phosphors are used in the form of fluorescent layers, often called screens, in conjunction with an optical detector (film, photocathode, photodiode) [1–3]. The performance of medical imaging systems is evaluated in terms of various parameters such as spatial resolution, quantum noise, signal-to-noise ratio (SNR) [2–5]. Evaluation is normally carried out on the integrated imaging detector.

In the present study, a method to evaluate the suitability of phosphor materials for use in medical imaging, is presented.

The method is based on the concept of noise-equivalent-quanta (NEQ) [5–8] expressing the fraction of incident X-ray quanta that are absorbed by a detector and used to create the final diagnostic image. NEQ has been also considered as an index of SNR and it has been defined as the square of the image SNR [7]. The latter is directly related to the X-ray dose incident on the detector. By the present method NEQ was expressed as a function of parameters associated with physical properties of the phosphor material independently of the optical detector used to capture the phosphor's light. The method was used to test three phosphors, namely  $\text{Y}_2\text{O}_2\text{S}:\text{Tb}$ ,  $\text{Y}_2\text{O}_2\text{S}:\text{Eu}$ , and  $\text{Y}_2\text{O}_3:\text{Eu}$ .  $\text{Y}_2\text{O}_2\text{S}:\text{Tb}$  and  $\text{Y}_2\text{O}_2\text{S}:\text{Eu}$  have the same chemical composition, that affects X-ray absorption, whereas  $\text{Y}_2\text{O}_2\text{S}:\text{Eu}$  and  $\text{Y}_2\text{O}_3:\text{Eu}$  have the same activator ( $\text{Eu}^{3+}$ ), that affects light wavelength and the intrinsic phosphor property to convert the absorbed X-rays into light.

## 1 Materials and methods

### 1.1 Derivation of NEQ formula

The optical signal  $S_P$  produced by a phosphor layer can be written as a function of spatial frequency ( $u$ ) as follows:

$$S_P(Q, u, w) = QC_P(Q, u, w), \quad (1)$$

where  $Q$  is the X-ray quantum fluence incident on the phosphor surface,  $w$  is the coating weight of the phosphor, and  $C_P$  expresses the contrast transfer function (CTF). The latter is used to describe the spatial frequency-dependent response of an imaging system to an input signal [4, 9]. CTF can be expressed as the product of the system's modulation transfer function (MTF), often used as an expression of spatial resolution, and the slope of its characteristic curve, often called the gradient [4, 5, 8, 9]. In the case of a phosphor layer, the gradient may be expressed as a conversion factor describing the efficiency of the phosphor to convert the incident X-ray

\* Corresponding author. Prof. D. Cavouras, Ph.D., 37-39 Esperidon Street, Kallithea 17671, Athens, Greece (Fax: +301/5910-975, E-mail: cavouras@hol.gr, cavouras@medisp.bme.teiath.gr)

quantum fluence  $Q$  into emitted optical quantum fluence  $\Phi_\lambda$ . The optical signal produced can then be written as:

$$S_p(Q, u, w) = Q \left[ \frac{d\Phi_\lambda(Q, w)}{dQ} \right] M_P(u, w), \quad (2)$$

where  $d\Phi_\lambda(Q, w)/dQ$  designates the aforementioned gradient and  $M_P$  is the MTF of the phosphor.

The output quantum noise associated with the optical quanta emitted by the phosphor can be described as a function of spatial frequency by the noise amplitude spectrum  $N_Q(u, w)$ , which is the square root of the noise power spectrum NPS [7, 10]. Thus, the spatial frequency-dependent signal-to-noise ratio can be expressed as:

$$\text{SNR}(Q, u, w) = Q \left[ \frac{d\Phi_\lambda(Q, w)}{dQ} \right] \frac{M_P(u, w)}{N_Q(u, w)}. \quad (3)$$

Considering that  $\text{NEQ} \equiv (\text{SNR})^2$  [7], the number of noise-equivalent quanta can then be written as follows:

$$\text{NEQ}(Q, u, w) = Q^2 \left[ \frac{d\Phi_\lambda(Q, w)}{dQ} \right]^2 \frac{[M_P(u, w)]^2}{W_Q(Q, u, w)}, \quad (4)$$

where  $W_Q$  is the quantum noise power spectrum (NPS) or Wiener spectrum associated with the number of emitted optical quanta.

Since the ratio  $d\Phi_\lambda/dQ$  expresses the efficiency of the phosphor material to convert incident X-ray quanta  $Q$  into emitted optical quanta  $\Phi_\lambda$ , relation (4) can be rewritten as follows:

$$\text{NEQ}(Q, u, w) = \frac{[\Phi_\lambda(Q, w)M_P(u, w)]^2}{W_Q(Q, u, w)}. \quad (5)$$

The quantum NPS has been expressed [10] as a function of  $\Phi_\lambda$  and  $M_P$  by the following relation:

$$W_Q(Q, u, w) = \Phi_\lambda(Q, w) [m(\lambda)M_P^2(u, w) + 1], \quad (6)$$

where  $m(\lambda)$  is the average number of optical quanta emitted per X-ray quantum absorbed in the phosphor. Relation (6) is valid under the assumption that the optical photons created within the phosphor material follow Poisson statistical distribution [10]. It must be also noted that  $Q$  and  $\Phi_\lambda$  represent mean numbers of quanta per unit area.

$\Phi_\lambda$  can be expressed in terms of the emitted optical energy fluence  $\Psi_\lambda$ , which is an easier measurable quantity, by the ratio:

$$\Phi_\lambda(Q, w) = \frac{\Psi_\lambda(Q, w)}{E_\lambda}, \quad E_\lambda = \frac{hc}{\lambda}, \quad (7)$$

where  $E_\lambda$  is the energy of an optical quantum,  $h$  is Plank's constant,  $c$  is the velocity of light, and  $\lambda$  is the wavelength of an optical quantum. Combining relations (4), (5), (6), and (7) NEQ can be written as:

$$\text{NEQ}(Q, u, w) = \frac{\Psi_\lambda(Q, w)\lambda}{hc} \left[ \frac{M_P^2(u, w)}{m(\lambda)M_P^2(u, w) + 1} \right]. \quad (8)$$

Relation (8) describes NEQ as a function of parameters strictly related to the phosphor material properties. These parameters can be determined by experimental measurements

and calculations. It must be also noted that  $\Psi_\lambda$  increases linearly with the number of incident X-ray quanta  $Q$ . This indicates that NEQ values will increase in a similar way with X-ray dose.

## 1.2 Experimental determination

The phosphors employed were in the form of fluorescent layers prepared in laboratory by sedimentation of the phosphor powder on fused silica substrates [11–13]. The mean size of the powder grains was approximately  $7 \mu\text{m}$ . Phosphor layers were prepared with coating weights ranging from approximately 20 to 200  $\text{mg}/\text{cm}^2$ . The phosphor materials used were  $\text{Y}_2\text{O}_2\text{S}:\text{Tb}$ ,  $\text{Y}_2\text{O}_2\text{S}:\text{Eu}$ , and  $\text{Y}_2\text{O}_3:\text{Eu}$ .

$\Psi_\lambda$  was measured in our laboratory using an EMI 9558 QB photomultiplier equipped with an extended E/S-20 photocathode and connected to a Carry 401 electrometer [11–14]. In the present study,  $\Psi_\lambda$  was measured during irradiation of the phosphor materials by X-rays using 50 kVp and 80 kVp X-ray tube voltages. Measurements were corrected by taking into account: (i) the spectral compatibility between the optical emission spectrum of the phosphor material and the spectral sensitivity of the photocathode of the photomultiplier, (ii) the geometric light collection efficiency of the photomultiplier, which depends on the phosphor–photocathode distance and on the angular distribution of the emitted light. Emission spectra and light angular distributions of the phosphor materials were also measured in our laboratory [11, 15]; spectra were measured by an Oriel 7240 grating monochromator and angular distributions were determined by previously described experimental techniques [15].  $M_P(u, w)$  was experimentally determined following the well-known square-wave response-function (SWRF) method [5, 12, 16]. To perform SWRF measurements a suitable test pattern (type 53, Nuclear Associates) was imaged by the light of the X-rayed phosphors on Agfa Scopix LT2B, for  $\text{Y}_2\text{O}_2\text{S}:\text{Eu}$  and  $\text{Y}_2\text{O}_3:\text{Eu}$ , and Agfa Curix Ortho GS, for  $\text{Y}_2\text{O}_2\text{S}:\text{Tb}$ , photographic emulsions. Pattern images were digitized by means of a Microtec Scanmaker II SP (24 bit color 1200×1200 dpi) scanner. MTF was then determined from the SWRF digitized images by Coltman's formula [5, 16].

$$M_P(u, w) = \frac{\pi}{4} \sum_{k=1}^{\infty} b_K \frac{\text{SWRF}[(2k-1)u, w]}{(2k-1)}, \quad (9)$$

where

$$b_K = 0, \quad \text{for } m < n, \\ b_K = (-1)^n (-1)^{k-1}, \quad \text{for } m = n.$$

$n$  is the number of prime factors other than unity in  $(2k-1)$ ,  $m$  is the number of prime factors other than unity which appear only once in  $(2k-1)$  [5]. The MTF determined by relation (9) was corrected for the scanner and film MTF as described previously [12].

The number  $m$  of optical photons emitted per absorbed X-ray quantum in (8) was determined by considering the relation:

$$m(\lambda) = \frac{\Phi_\lambda(Q, w)}{\eta_A(\mu_X, w)Q} = \frac{\lambda}{hc} \frac{\Psi_\lambda(Q, w)}{\eta_A(\mu_X, w)Q}, \quad (10)$$

where  $\eta_A$  is the fraction of X-rays absorbed by the phosphor material, calculated considering that X-ray absorption follows the exponential law. The X-ray absorption coefficients  $\mu_X$  were calculated from data given by Storm and Israel [12, 17].  $Q$  was determined from exposure measurements using a PTW dosimeter (ionization chamber type No. 23333).

## 2 Results and discussion

Figures 1 and 2 show the variation of NEQ with spatial frequency for 50 mg/cm<sup>2</sup> and 80 mg/cm<sup>2</sup> phosphor layers determined at 50 kVp and 80 kVp, respectively. The corresponding values of  $Q$  (X-ray dose) were  $0.15 \times 10^6$ ,  $1.12 \times 10^6$  X-ray quanta/cm<sup>2</sup>. NEQ falls off rapidly with frequency and this behaviour is more pronounced for Y<sub>2</sub>O<sub>3</sub>:Eu. The variation of NEQ with spatial frequency is principally determined by the modulation transfer function  $M_P(u, w)$  in formula (8), which is shown in Fig. 3. MTF is the Fourier transform of the point spread function (PSF), which degrades with the thickness of the phosphor layer and depends strongly on the optical attenuation properties of the material. For equal coating weight, the Y<sub>2</sub>O<sub>3</sub>:Eu phosphor layer is thicker than Y<sub>2</sub>O<sub>2</sub>S:Tb and Y<sub>2</sub>O<sub>2</sub>S:Eu due to the higher dens-

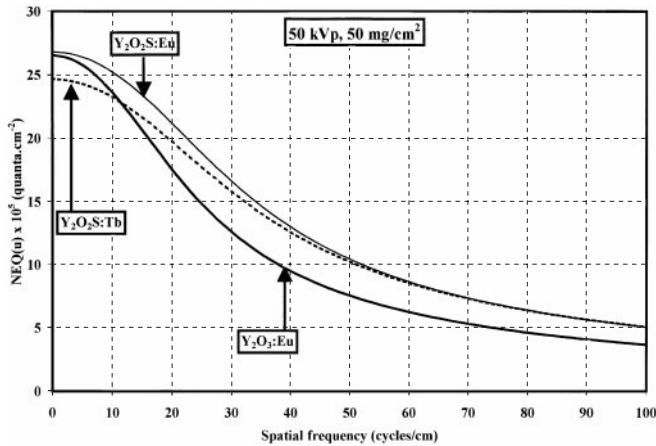


Fig. 1. Variation of noise-equivalent quanta (NEQ) with spatial frequency, determined at 50 kVp X-ray tube voltage for 50-mg/cm<sup>2</sup> phosphor layers

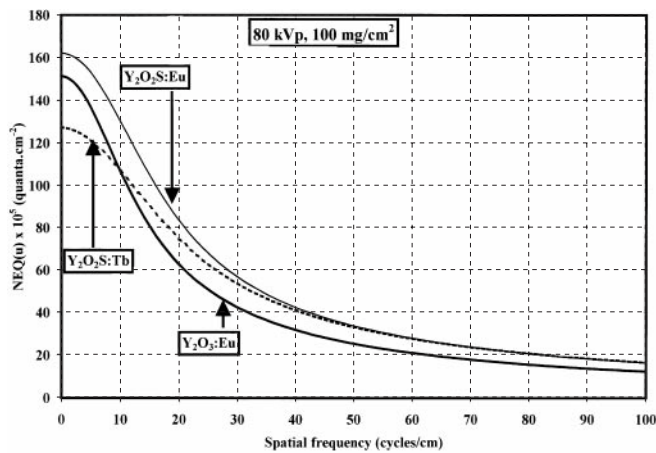


Fig. 2. Variation of noise-equivalent quanta (NEQ) with spatial frequency, determined at 80 kVp X-ray tube voltage for 100-mg/cm<sup>2</sup> phosphor layers

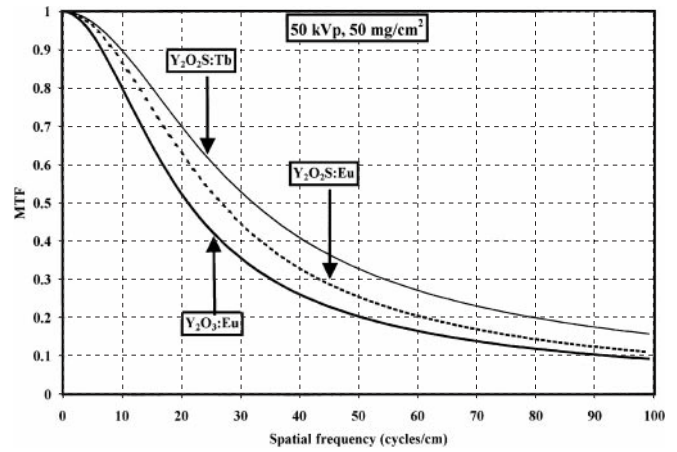


Fig. 3. MTF curves for 50-mg/cm<sup>2</sup> phosphor layer measured at 50 kVp X-ray tube voltage

ity of the latter (5 g/cm<sup>3</sup> for Y<sub>2</sub>O<sub>2</sub>S:Tb or Y<sub>2</sub>O<sub>2</sub>S:Eu against 2.2 g/cm<sup>3</sup> for Y<sub>2</sub>O<sub>3</sub>:Eu). Thus, in the case of Y<sub>2</sub>O<sub>3</sub>:Eu, optical quanta generated at a point within the phosphor travel longer distances to arrive at the layer's surface. Since light is isotropically produced in space, the laterally directed quanta spread into a surface area that increases with the length of optical trajectories. This effect augments the width of PSF resulting in lower MTF values for Y<sub>2</sub>O<sub>3</sub>:Eu.

For equal thickness at equal coating weight, as is the case of Y<sub>2</sub>O<sub>2</sub>S:Tb and Y<sub>2</sub>O<sub>2</sub>S:Eu phosphors, the MTF differences between the two materials are due to differences in their optical attenuation properties. The importance of optical attenuation increases with frequency of light, which is higher for the blue-green-emitting Y<sub>2</sub>O<sub>2</sub>S:Tb than for the red-emitting Y<sub>2</sub>O<sub>2</sub>S:Eu. Thus, laterally directed optical quanta suffer more attenuation in Y<sub>2</sub>O<sub>2</sub>S:Tb than in Y<sub>2</sub>O<sub>2</sub>S:Eu. This attenuation restricts the area of light spread in the phosphor's surface resulting in sharper PSF and better MTF values for Y<sub>2</sub>O<sub>2</sub>S:Tb than for Y<sub>2</sub>O<sub>2</sub>S:Eu.

At the low-frequency range, MTF values tend to unity for all phosphors, hence the influence of MTF on NEQ values is not so important. Low- and medium-frequency NEQ is then mainly determined by the ratio  $\Psi_\lambda/E_\lambda$ .  $\Psi_\lambda$  was found approximately equal for Y<sub>2</sub>O<sub>2</sub>S:Tb and Y<sub>2</sub>O<sub>2</sub>S:Eu and slightly lower for Y<sub>2</sub>O<sub>3</sub>:Eu. This difference may be principally explained by the lower X-ray absorption of Y<sub>2</sub>O<sub>3</sub>:Eu due to its lower effective atomic number and density. However,  $E_\lambda$  is lower in the cases of Y<sub>2</sub>O<sub>2</sub>S:Eu and Y<sub>2</sub>O<sub>3</sub>:Eu (higher  $\lambda$ ), which both emit red light, than in Y<sub>2</sub>O<sub>2</sub>S:Tb and, hence, the product  $\Psi_\lambda E_\lambda$  is improved in the Eu<sup>3+</sup> activated phosphors. This explains the superiority of Y<sub>2</sub>O<sub>2</sub>S:Eu NEQ in the medium- to low-frequency range from 0 to 50 cycles/cm and the superiority of Y<sub>2</sub>O<sub>3</sub>:Eu over Y<sub>2</sub>O<sub>2</sub>S:Tb in the very low frequency range below 15 cycles/cm.

Figure 4 shows the variation of zero-frequency NEQ with coating weight. NEQ values initially increase towards a maximum value and decrease thereafter. This type of variation is determined by  $\Psi_\lambda$ , which in turn is determined by the X-ray absorption of the phosphor and the fraction of light transmitted through the phosphor layer and escaping from its surface [18]. The increasing part of NEQ curves is principally affected by the X-ray absorption that initially increases with coating weight but gradually tends towards a constant

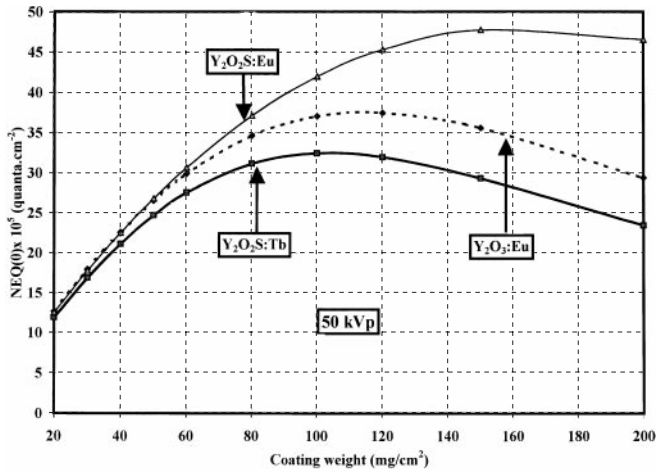


Fig. 4. Variation of zero-frequency noise-equivalent quanta (NEQ(0)) with phosphor coating weight, determined at 50 kVp X-ray tube voltage

value at thick phosphor layers. On the other hand, the fraction of optical quanta transmitted through the phosphor decreases at high coating weights due to the importance of optical attenuation effects during light passage through thick phosphor layers. This effect reduces  $\psi_\lambda$  and determines the decreasing part of the NEQ curves at high coating weights. However, the decrease of the  $Y_2O_2S:Eu$  NEQ was found considerably slower as compared to  $Y_2O_2S:Tb$ . This may be explained by considering that the fraction of transmitted optical quanta is higher in  $Y_2O_2S:Eu$ , because optical attenuation effects are less important in this phosphor. Optical attenuation is also less important in  $Y_2O_3:Eu$ , also emitting lower frequency red light, and hence NEQ is higher for  $Y_2O_3:Eu$  as compared to  $Y_2O_2S:Tb$  at high coating weights.

Figure 5 shows NEQ variation with coating weight at 20 cycles/cm. The peak values of NEQ were obtained at considerably lower coating weights than in the case of zero frequency NEQ (see Fig. 4). This is due to the influence of MTF which falls off with thickness and hence with coating weight. This effect modifies the shape of NEQ curves which

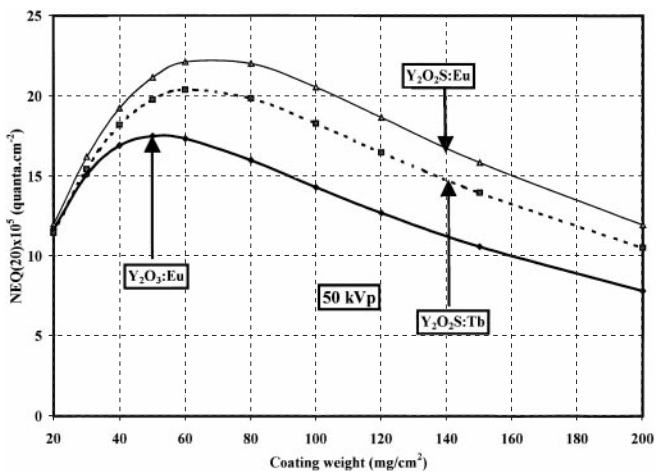


Fig. 5. Variation of noise-equivalent quanta at 20 cycles/cm spatial frequency (NEQ(20)) with phosphor coating weight, determined at 50 kVp X-ray tube voltage

then start to decrease at lower coating weights. Additionally the effect of MTF improves the performance of  $Y_2O_2S:Tb$  which, due to its higher MTF, is now better than  $Y_2O_3:Eu$  and closer to  $Y_2O_2S:Eu$ . The relative position of the three curves in Fig. 5 is in accordance with data shown in Fig. 1 at frequency 20 cycles/cm. Finally, it has to be emphasized that NEQ augments linearly with the number of incident X-ray quanta (X-ray dose). However, for a certain value of X-ray tube voltage (kVp), the number of X-rays was equal for all measurements. Thus, any dose modification under the same tube voltage conditions such as an increase in the tube current will alter NEQ values by the same factor and, hence, the relative curve position will not be affected.

### 3 Summary

A method is presented using the number of noise-equivalent quanta to evaluate the imaging performance of phosphor materials. NEQ was expressed as a function of the following measurable quantities: emitted optical flux, wavelength and MTF, which depend on material physical properties such as effective atomic number, density, type of activator, and optical attenuation properties. The advantage of the method is that it evaluates phosphor materials independently of the optical detector used in conjunction with phosphors in medical imaging systems. From the phosphor materials tested,  $Y_2O_2S:Eu$  was found to exhibit highest NEQ values, although it had inferior MTF than  $Y_2O_2S:Tb$ . NEQ values of  $Y_2O_3:Eu$  were found close to  $Y_2O_2S:Eu$  at low frequencies.

*Acknowledgements.* This study is dedicated to the memory of Prof. G.E. Giakoumakis, leading member of our team, whose work on phosphor materials has inspired us to continue.

### References

1. G. Zweig, D.A. Zweig: Proc. SPIE **419**, 297 (1983)
2. P. Haque, J.H. Stanley: In *Radiology of the Skull and Brain Technical Aspects of Computed Tomography* (C.V. Mosby, St. Louis, MO 1981) p. 4103
3. M.J. Yaffe, J.A. Rowlands: Phys. Med. Biol. **42**, 1 (1997)
4. P.C. Bunch, K.E. Huff, R. Van Metter: J. Opt. Soc. Am. **4**, 902 (1987)
5. ICRU: Modulation Transfer Function of Screen-film Systems, ICRU Report 41 (1986)
6. J.C. Dainty, R. Shaw: In *Image Science* (Academic Press, New York 1974) pp. 152–188
7. W. Hillen, U. Schiebel, T. Zaengel: Med. Phys. **14**, 744 (1987)
8. R. Van Metter, R. Dickerson: Med. Phys. **21**, 1483 (1994)
9. R. Van Metter: Med. Phys. **19**, 53 (1992)
10. R. Shaw, R. Van Metter: Proc. SPIE **454**, 128 (1984)
11. G. Panayiotakis, D. Cavouras, I. Kandarakis, C. Nomicos: Appl. Phys. A **62**, 483 (1996)
12. D. Cavouras, I. Kandarakis, G. Panayiotakis, E.K. Evangelou, C.D. Nomicos: Med. Phys. **23**, 1965 (1996)
13. I. Kandarakis, D. Cavouras, G. Panayiotakis, T. Agelis, C. Nomicos, G. Giakoumakis: Phys. Med. Biol. **41**, 297 (1996)
14. D. Cavouras, I. Kandarakis, G.S. Panayiotakis, E. Kanellopoulos, D. Triantis, C.D. Nomicos: Appl. Radiat. Isot. **49**, 931 (1998)
15. G.E. Giakoumakis, D.M. Miliotis: Phys. Med. Biol. **30**, 21 (1985)
16. G.T. Barnes: In *The Physics of Medical Imaging: Recording System, Measurements and Techniques*, ed. by A.G. Haus (American Association of Physicists in Medicine, New York 1979) pp.138–151
17. E. Storm, H. Israel: Report LA-3753: Los Alamos Scientific Laboratory, University of California. 1967
18. G.W. Ludwig: J. Electrochem. Soc. **118**, 1152 (1971)